A comprehensive investigation of the peak capacity for the reversed-phase gradient liquid-chromatographic analysis of intact proteins using a polymer-monolithic capillary column

Fernandez-Pumarega, Alejandro; Dores-Sousa, Jose Luis; Eeltink, Sebastiaan

Published in:
Journal of Chromatography A

DOI:
10.1016/j.chroma.2019.460462

Publication date:
2020

A comprehensive investigation of the peak capacity for the reversed-phase gradient liquid-chromatographic analysis of intact proteins using a polymer-monolithic capillary column

Alejandro Fernández-Pumarega[1‡], José Luís Dores-Sousa[2‡], Sebastiaan Eeltink[2,*]

[1]Departament d'Enginyeria Química i Química Analítica and Institut de Biomedicina (IBUB), Facultat de Química, Universitat de Barcelona, Barcelona, Spain

[2]Vrije Universiteit Brussel (VUB), Department of Chemical Engineering, Brussels, Belgium

(‡) These authors contributed equally to this work.

(*) Corresponding author

Pleinlaan 2, B-1050, Brussels, Belgium

Tel.: +32 (0)2 629 3324, Fax: +32 (0)2 629 3248, E-mail: sebastiaan.eeltink@vub.be

Highlights:

- The maximum peak capacity is achieved at a flow rate 20 x higher than the optimal van Deemter flow rate
- The gradient volume has an important impact on overall peak capacity
- The use of TFA as ion-pairing agent leads to better mass loadability compared to FA

Abstract

The present study reports on the analysis of different factors affecting the magnitude of the peak capacity for intact protein separations conducted in gradient reversed-phase liquid chromatography. Experiments were conducted using a 200 µm i.d. capillary styrene-*co*-divinylbenzene monolithic column that was developed in-house and was characterized by a mode globule cluster size of 1.2 µm and a mode macropore size of 1.0 µm (based on scanning electron microscopy). The monolith yielded a minimum plate-height value of 13.3 µm for uracil. The use of trifluoroacetic acid instead of formic acid as ion-pairing agent generally led to better peak symmetry, narrower peak widths which effect is protein-dependent, and improved loadability characteristics. The peak capacity has been systematically assessed at different flow rates and gradient duration. The highest peak capacity of 247 was obtained at a flow rate of 1 µL·min^{-1} and a gradient time of 120 min, which corresponds to an optimal t_G/t_0 ratio of ~60. While the optimum van Deemter velocity for intact proteins was approximated to be 0.065 µL·min^{-1}, the highest peak capacity was achieved at approximately 20-fold higher flow rate, depending on the gradient duration applied and the molecular weight of the proteins. The optimum velocity increased with decreasing gradient time and is a compromise between the magnitude of the mass-transfer contribution (decreasing the peak capacity with velocity) affect by molecular diffusion, and the increase in peak capacity induced by the more favorable gradient-volume ratio.

Keywords: kinetic performance; van Deemter; ion-pairing agent; loadability; top-down proteomics.

1. Introduction

The chromatographic analysis of intact proteins is becoming increasingly important. This is in part because of regulatory guidelines that demand for the comprehensive characterization of emerging biotherapeutics, such as monoclonal antibodies and antibody-drug conjugates, with respect to the primary sequence, impurity profiles including posttranslational modifications, and also higher order structures [1–3]. Reversed-phase gradient LC is the workhorse for protein analysis, allowing the analysis of proteins that cover broad hydrophobicity range and that adequately considers the steep dependency of retention factor and mobile-phase composition using columns are packed with large-pore (300 – 1000 Å) silica C_4-modified particles [4,5]. Capillary column formats are readily interfaced to mass spectrometry via electrospray interfacing. Furthermore, current top-down mass-spectrometry approaches provide reliable sequence information and databases enabling automated protein identifications are rapidly expanding [6]. Examples of the current state-of-the-art intact protein separations comprise the work of Wagner *et al.* who designed superficially porous C_4-particles with wide large-pores (1000 Å) for separation of large biomolecules [4] , Shen *et al.* reported the use of $\geq$ 1 meter-long C_4-core-shell (200-300 Å) columns for top-down proteomics, obtaining high-resolution separations of the proteoforms of a microbial lysate [7], and Kirkland *et al.*, showing fast separations of protein mixtures of 9 and 5 different proteins in less than 2 and 0.33 minutes, respectively, using core-shell particle packed columns [8].

Polymer-monolithic stationary phases, characterized by interconnected (micro)globular support structure percolated with macropores, have been introduced in 1989 as a viable alternative for protein analysis with packed columns [9]. In this year Svec *et al.* also demonstrated separation of four intact proteins in 30 s operating large column conduits in RP-LC mode applying a flow rate of 25 mL/min in 1993 [10]. The development of capillary column formats containing poly(styrene-*co*-divinylbenzene) entities by Huber *et al.* yielding exquisite

separation efficiency is considered a breakthrough in technology, allowing hyphenation of monolith chromatography to mass spectrometric detection [11,12]. In 2014, Vaast *et al.* demonstrated the development of polymer monolithic nanomaterials compatible with ultra-high pressures allowing for high-resolution protein and peptide gradient separations within sub-minute analysis times [13,14].

To assess the separation performance in gradient mode, peak capacity has been introduced as metric, which is defined as the number of peaks that fit within the gradient window with a fixed resolution [15]. However, to resolve 98% of the analytes that are randomly distributed over the gradient window, the peak capacity must exceed the number of components in the sample by a factor of 100 [16–18]. In an excellent paper, Neue derived a general theoretical model to describe peak capacity for small molecule separations in isocratic and gradient reversed-phase LC mode based on the linear solvent strength (LSS) retention model and peak dispersion induced by the eddy dispersion (*A*-term), longitudinal diffusion (*B*-term), and mass-transfer (*C*-term) contributions [19]. This model was then extended to describe the peak capacity for a wide range of analytes, including peptides, oligonucleotides and oligomers [20–22]. Different experimental studies have been performed in RP-LC mode aiming at maximizing the peak capacity for biomolecule separation [22–25]. Marchetti *et al.* optimized gradient RP-LC analysis of peptides and concluded that to operate in the relatively low optimal velocity (u_{opt}) also relatively low gradient volume should be applied [23]. In contrast, Wang *et al.* reported the maximum peak capacity is generated when applying a flow rate higher than u_{opt} [24] and this observation was later confirmed by Petersson *et al.* for small-molecule and peptide separations [25], and also Neue and Gilar for oligonucleotide separations [22].

The current study focusses on the comprehensive characterization and optimization of the gradient performance for intact protein separations with respect to peak capacity using a capillary polymer-monolithic column prepared from polystyrene and divinylbenzene. First,

optimization of system conditions and effect of ion-pairing agents (type and concentration) are discussed. Next, the effects of flow rate and gradient volume on resulting peak capacity were assessed and the validity of Neue's peak capacity model for intact protein analysis was investigated. The effect of molecular weight on the selection of optimal gradient conditions is discussed. Finally, the potential of monolith chromatography for profiling intact proteins and degradation products is demonstrated at optimal gradient conditions.

2. Materials and methods

2.1. Chemicals and materials

2,2'-azobis(2-methylpropionitrile) (AIBN, 98%), 1-decanol (≥ 98%), divinylbenzene (DVB, 80%), styrene (S, ≥ 99%), tetrahydrofuran (THF, anhydrous, inhibitor-free, ≥ 99.9%), toluene (anhydrous, 99.8%), 3-(trimethoxysilyl)propyl methacrylate (98%), and proteins including carbonic anhydrase from bovine erythrocytes (≥ 95%), cytochrome *c* from bovine heart (≥ 95%), cytochrome *c* from equine heart (≥ 95%), insulin from bovine pancreas, lysozyme from chicken egg white (≥ 90%), myoglobin from equine heart (≥ 90%), and ribonuclease A from bovine pancreas were purchased from Sigma-Aldrich (Zwijndrecht, The Netherlands). Aluminium oxide (90 active neutral), hydrochloric acid (32%) and sodium hydroxide pellets, and uracil were purchased from Merck (Darmstadt, Germany). Acetonitrile (ACN, HPLC supra-gradient quality), formic acid (FA, 99%) and trifluoroacetic acid (TFA, 99%) were purchased from Biosolve (Valkenswaard, The Netherlands). Deionized water (18.2 MΩ.cm) was purified in-house using a Milli-Q water-purification system (Millipore, Molsheim, France). Polyimide-coated fused-silica capillary tubing (200 µm i.d. × 350 µm o.d.) was purchased from Polymicro Technologies (Molex B.V, Eindhoven, The Netherlands).

2.2. Synthesis of polymer-monolithic capillary columns

To establish a covalent link between the monolithic entity and the capillary wall preventing channeling effects, a surface-modification procedure was followed as previously described in [26]. In summary, the procedure includes *i*) regeneration of silanol groups by flushing the capillary subsequently with 1 M sodium hydroxide solution during 30 minutes at 2 $\mu L \cdot min^{-1}$, flushing with water, and flushing with 1 M hydrochloric acid solution at 2 $\mu L \cdot min^{-1}$ during 30 minutes; *ii*) surface modification by flushing the capillary with a solution containing 10% (v/v) 3-(trimethoxysilyl)propyl methacrylate diluted in toluene during 1 hour at 2 $\mu L \cdot min^{-1}$; and *iii*) removal of unreacted monomer by flushing with toluene. After each flushing step the capillary was dried with air. After completing surface modification, the capillary was filled with the monolithic precursor mixture, composed of 2 wt% AIBN (the initiator), 20 wt% S and 20 wt% DVB (the monomer and the crosslinking monomer, respectively), and a solution of THF and 1-decanol (the porogen), with a monomer to porogen ratio of 40:60 wt%. The polymerization reaction was carried out in a water bath maintained at 70ºC for 24 hours to reach complete conversion. After completion of the polymerization reaction, the column was rinsed with ACN.

2.3. Instrumentation and LC conditions

Gradient LC experiments were performed employing an Ultimate 3000 HPLC system (Thermo Fisher Scientific, Germering, Germany) consisting on a dual-ternary pump with a degasser module, a column oven equipped with a 1:100 flow splitter, a well-plate autosampler, and a UV detector with a 3 nL detector flow cell. The connections between the flow splitter, the injection valve and the column were established using 20 µm i.d. fused-silica capillaries. Mobile phase A consisted of 0.1% (v/v) aqueous TFA or FA and mobile phase B of 80:20%

(v/v) ACN:water with 0.08% (v/v) TFA or FA. The protein test mixture contained 1-2 $\mu g \cdot mL^{-1}$ of ribonuclease A, insulin, myoglobin, lysozyme, carbonic anhydrase, and cytochrome *c* from bovine and equine, dissolved in mobile phase A. The gradient window was from 25-60 %B, corresponding to $\Delta c = 0.28$.

All gradient separations were performed using a "direct injection" set-up applying a 1 µL full-loop injection. The column was placed in the column oven thermostated at 37ºC. UV detection was performed at 210 nm, with a 20 Hz data collection rate and 0.12 s response time. Isocratic experiments were conducted to determine the separation efficiency with a 20 nL injection valve and direct attachment of the column on to the valve stator. The capillary column was connected to a 3 nL flow cell equipped with 20 µm i.d. × 100 mm long inlet tubing. Uracil was used as a void (t_0) marker applying 100% mobile phase B.

3. Results and discussion

A polymer styrene-*co*-divinylbenzene monolithic entity was synthesized *in-situ* in a capillary column format with 200 µm i.d., applying a thermally initiated free-radical polymerization. Fig. 1 shows the interconnected globular structure of a high-porosity monolith prepared with a monomer to porogen ration of 40/60 w%. The monolith, covalently linked to the column wall, spans the cross section and a seemingly homogeneous structure has been obtained. Based on scanning electron micrographs we estimate that the interconnected polymer agglomerates are approximately 1.2 µm in diameter and the macropores 1.0 µm obtained from at least 100 measurements, see Fig. S1. The minimum plate height (H_{min}) was determined by injection of uracil used as void marker to be 13.3 µm, with van Deemter characteristics $A = 5.9$ µm, $B = 1.8$ mm^2/s, and $C_m = 7.1$ ms, as determined via non-linear regression, see Fig. S2. The Van Deemter curve for an intact protein with a molecular weight of 22.7 kDa was reconstructed

taking into account the molecular diffusion coefficient. The permeability ($K_{v,0}$) was determined based on the Darcy equation to be $7.73 \cdot 10^{-15}$ m^2.

Ion-pairing chromatography in RP-LC mode is commonly used to retained ionized biomolecules by the hydrophobic stationary phase. First, the tubing i.d. and flow-cell volume were optimized to minimize the extra-column contribution to band broadening. The effects of type (FA *versus* TFA) and concentration of the ion-pairing agent on protein retention, peak shape, and peak width are demonstrated in Fig. 2. Fig. 2A shows the effect of type of ion-pairing agent applying the same concentration (0.1%) and gradient span ($\Delta c = 0.28$). Applying TFA instead of FA increases protein retention, due to the formation of strong ion pairs, which is expected based on the pK_a values (0.23 for TFA *versus* 3.75 for FA). Note, the peak profile of lysozyme was significantly degraded, when FA was used. This seems to be a protein specific effect. Compared to columns packed with porous particles the surface area of polymer monoliths is significantly lower a factor 6 up to 8 depending on the size, number, and agglomeration level of the polymer globules [27], which impairs the loadability. Fig. 2B shows a zoom-in of peak profiles obtained when increasing the injected protein concentration from 1 ppm, to 5 ppm, up to 10 ppm (applying 1 µL full-loop injections). Up to 2.5 ppm the peak width was not affected. Above this threshold the peak width increases linearly with protein mass, but symmetric peak shape was still observed up to 10 ppm. Even when injecting 50 ppm, no carry-over could be detected in the UV trace of subsequent blank gradient runs, which is independent of the type of ion-pairing agent applied. The use of FA negatively influences mass loadability; when injecting 10 ppm insulin an 81% increase in peak width was observed when using 0.1% FA, while only a 19% increase in peak width was observed using TFA as the ion-pairing agent (data not shown).

A model to approximate the peak capacity (n_c) of peptides in gradient mode derived by Neue shows that the peak capacity depends on the gradient steepness defined as the ratio of the

gradient time and the column dead time (t_G/t_0) the solvent-strength parameter (S), and of the column efficiency (N), according to [22]:

$$n_c = 1 + \frac{\sqrt{N}}{4} \cdot \frac{S \cdot \Delta c}{S \cdot \Delta c \cdot \frac{t_0}{t_g} + 1} \quad (1)$$

where S is defined as the slope of the linear dependency of ln k *versus* the volume fraction of organic solvent in the mobile phase. S values ranged between 131.9 for carbonic anhydrase (MW ~ 30.0 kDa) and 48.5 for insulin (MW ~ 5.8 kDa), respectively, see Fig. S3. The isocratic plate count (N) can be expressed as a function of operating parameter, *i.e.*, column length (L), and domain size (d_{dom}) approximated as the sum of the mode globule size and mode macropore size, and the (reduced) a-, b-, and c_m-term contributions of the van Deemter equation:

$$N = \frac{L}{a \cdot d_{dom} + \frac{b \cdot D_m \cdot t_0}{L} + c_m \cdot \frac{{d_{dom}}^2}{D_m} \cdot \frac{L}{t_0}} \quad (2)$$

where D_m is the diffusion coefficient. Note that the convective transport in a monolith (or any support structure operated at laminar flow conditions) occurs parallel with the surface. Also, the stationary-phase mass-transfer contribution (C_s-term) is merely absent, since this type of polymer monolith contains a very limited fraction of meso- and micropores, and these pores are generally not accessible for large molecules [28] .

The gradient performance was assessed for the separation of a mixture of intact proteins with molecular weights ranging between 5.8 - 22.7 kDa, yielding diffusion coefficients between 12 and 9×10^{-11} $m^2 \cdot s^{-1}$, based on the methodology of laminar flow analysis [29]. The gradient time and flow rate were systematically varied and the corresponding experimental peak capacities were determined from the average peak width at half height ($W_{1/2}$) recorded for mixture of 7 proteins. A linear increase in peak width was obtained as function of gradient time (independent of flow rate), resulting in a steep initial increase in peak capacity between t_G 5-

60 min, and at longer gradient times the peak capacity increase levels off, see Fig S4. A maximum peak capacity of 250 was observed applying a gradient time of 120 min. Although the peak capacity can be moderately increased by using longer gradient duration, such a gain in overall performance can only obtained at the expense of a significantly lower peak production rate (peak-capacity-per-unit time). Fig. 3 shows the average peak capacity as function of the flow rate and applying different gradient duration (between 10 min and 120 min). Fig. S5A and B shows the data for carbonic anhydrase and insulin. The trendline has been constructed based on Eqs. 1 and 2 with the van Deemter parameters, determined for uracil and recalculated based on reduced *a*-, *b*-, and *c*-terms and considering the diffusion coefficients and experimentally-determined *S* value. Neue's model provides a reasonable estimation for carbonic anhydrase, however the experimental peak capacities for insulin are much higher than predicted for insulin. Note that Neue's model assumes the validity of the linear solvent-strength (LSS) model to describe protein retention, which may lead to a significant underestimation of *S*, which in turn leads to an underestimation of n_c.

Fig. 3 shows that fixing the flow rate and increasing t_G leads to a higher peak capacity, as predicted by Eq. 1. The representation depicted in Fig. 3 also shows that the maximum peak capacities are reached when applying flow rates of 1 µL·min^{-1} or higher, and that the optimal mobile-phase velocity yielding maximum peak capacity strongly depends on gradient duration applied. The optimum flow rate at a gradient duration of 120 min was obtained at a flow rate of 1 µL·min^{-1}, which corresponds to an optimal t_G/t_0 ratio of ~60. The optimum velocityincreases with decreasing gradient time. The optimal volumetric flow rate (F_{opt}) when applying a gradient of 10 min was observed at 2 µL·min^{-1}, which corresponds to an optimal t_G/t_0 ratio of ~10. The effect of flow rate on peak capacity was also assessed for individual proteins, *i.e.*, carbonic anhydrase (MW = 30.0 kDa), ribonuclease A (MW = 13.7 kDa), and insulin (MW = 5.8 kDa). The optimal mobile-phase velocity depends on the molecular weight.

With increasing molecular weight D_m decreases and the optimal flow velocity (F_{opt}) shifts to low velocity, as can be expected based on the van Deemter curve.

To assess the effect of flow rate on N, which in turn affects the magnitude of n_c the average peak capacity is plotted as function of t_G/t_0, while operating the column at different flow rates, see Fig. 4A. When comparing the performance at a fixed t_G/t_0 value, *i.e.*, $t_G/t_0 = 30$, it is observed that the peak capacity decreases when applying higher flow rates. This effect can be mainly attributed to the effect of mobile-phase velocity on the magnitude of the mobile-phase mass-transfer (C_m-term) contribution. Based on the van Deemter data depicted in Fig. S2 it is anticipated that the optimum van Deemter flow rate for intact proteins is reached at a flow rate below 0.1 µL·min^{1}. Hence, at flow rates of 0.5 µL·min^{-1} and above, the column is operated in the C-term region of the van Deemter curve. When plotting the (σ·flow rate)^2 values, that are proportional to apparent plate height, as function of flow rate (see Fig. 4B) an increase in the slope is observed, representing the resistance to mass transfer (C-term) contributions in gradient mode for three individual proteins, *i.e.*, carbonic anhydrase, ribonuclease A, and insulin. With increasing molecular weight an increase in slope is observed, as the plate height in the C-term region of the van Deemter curve is inversely proportional to D_m. Note that the molecular-diffusion coefficients do not correlate with the apparent efficiency, see also Fig. S6 for a wider range of intact proteins. Fig. 4B also demonstrates that the gradient volume, defined by the gradient span (Δc) and the t_G/t_0 ratio, has a large effect on the resulting peak variance.

Fig. 5 shows the potential of the capillary polymer-monolithic columns for profiling intact proteins and their impurities/degradation products, yielding an average peak capacity of 247. The separation was conducted at a flow rate of 1 µL·min^{-1}, applying a gradient time of 120 minutes, and optimizing Δc (= 0.28) to maximize peak coverage within the gradient span. The zoom-in between the 30- and 70-min timeslot demonstrates the very-high resolving power.

4. Concluding remarks

The peak capacity in gradient LC is a trade-off between, on the one hand, the flow rate affecting the peak capacity via the plate number, and on the other hand the effect of flow rate affecting the gradient volume, defined by t_G/t_0. To maximize the peak capacity in gradient mode the use of faster than optimal (van Deemter) flow rates is encouraged, since this effectively leads to shallower gradients. In our study, the highest peak capacity for intact proteins in gradient mode applying the monolithic capillary column was achieved at flow rates a factor 10-20 higher than u_{opt}. By using a highly-efficient monolithic column, the mass transfer (C-term) contribution to band broadening is relatively low. Hence, the loss in efficiency at elevated flow rates is only modest, and also depends on the diffusion coefficient of the proteins. Note that the resulting peak capacity also depends on gradient slope. At a flow rate of 1 µL·min^{-1} and a gradient time of 120 min, the magnitude of the peak capacity is dominated by the effect of gradient volume. When increasing the flow rate further, the peak capacity decreases because of the dominating *C*-term contribution to band broadening. When applying short 10 min gradients the optimal gradient flow rate is reached at 2 µL·min^{-1}. With other words, for very shallow gradients, the optimal flow rate approaches the optimal van Deemter flow rate as measured in isocratic mode.

5. Acknowledgements

JLDS and SE acknowledge grants of the Research Foundation Flanders (FWO – grant no. G025916N and G033018N). AFP wishes to thank the University of Barcelona for his APIF PhD fellowship. The authors thank Dr. Martin Gilar (Waters Corporation, Milford, USA) for helpful discussions.

6. References

[1] A. Wagh, H. Song, M. Zeng, L. Tao, T.K. Das, Challenges and new frontiers in analytical characterization of antibody-drug conjugates, MAbs. 10 (2018) 222–243.

[2] European Medicines Agency, Guideline on development, production, characterisation and specification for monoclonal antibodies and related products. https://www.ema.europa.eu/en/development-production-characterisation-specifications-monoclonal-antibodies-related-products, 2016 (accessed 01 May 2019).

[3] M. Tassi, J. De Vos, S. Chatterjee, F. Sobott, J. Bones, S. Eeltink, Advances in native high-performance liquid chromatography and intact mass spectrometry for the characterization of biopharmaceutical products, J. Sep. Sci. 41 (2018) 125–144.

[4] B.M. Wagner, S.A. Schuster, B.E. Boyes, T.J. Shields, W.L. Miles, M.J. Haynes, R.E. Moran, J.J. Kirkland, M.R. Schure, Superficially porous particles with 1000 Å pores for large biomolecule high performance liquid chromatography and polymer size exclusion chromatography, J. Chromatogr. A. 1489 (2017) 75–85.

[5] S.A. Schuster, B.M. Wagner, B.E. Boyes, J.J. Kirkland, Optimized superficially porous particles for protein separations, J. Chromatogr. A. 1315 (2013) 118–126.

[6] J.S. Cottrell, Protein identification using MS/MS data, J. Proteomics. 74 (2011) 1842–1851.

[7] Y. Shen, N. Tolić, P.D. Piehowski, A.K. Shukla, S. Kim, R. Zhao, Y. Qu, E. Robinson, R.D. Smith, L. Paša-Tolić, High-resolution ultrahigh-pressure long column reversed-phase liquid chromatography for top-down proteomics, J. Chromatogr. A. 1498 (2017) 99–110.

[8] J.J. Kirkland, F.A. Truszkowski, C.H. Dilks Jr., G.S. Engel, Superficially porous silica microspheres for fast high-performance liquid chromatography of macromolecules, J. Chromatogr. A. 890 (2000) 3–13.

[9] F. Svec, Monolithic columns: A historical overview, Electrophoresis. 38 (2017) 2810–2820.

[10] Q.C. Wang, F. Svec, J.M.J. Fréchet, Macroporous polymeric stationary-phase rod as continuous separation medium for reversed-phase chromatography, Anal. Chem. 65 (1993) 2243–2248.

[11] H. Oberacher, C.G. Huber, Capillary monoliths for the analysis of nucleic acids by high-performance liquid chromatography-electrospray ionization mass spectrometry, TrAC - Trends Anal. Chem. 21 (2002) 166–174. doi:10.1016/S0165-9936(02)00304-7.

[12] A. Premstaller, H. Oberacher, W. Walcher, A.M. Timperio, L. Zolla, J. Chervet, N. Cavusoglu, A. Van Dorsselaer, C.G. Huber, High-performance liquid chromatography − electrospray ionization mass spectrometry using monolithic capillary columns for proteomic studies, Anal. Chem. 73 (2001) 2390–2396.

[13] A. Vaast, E. Tyteca, G. Desmet, P.J. Schoenmakers, S. Eeltink, Gradient-elution parameters in capillary liquid chromatography for high-speed separations of peptides and intact proteins, J. Chromatogr. A. 1355 (2014) 149–157.

[14] A. Vaast, H. Terryn, F. Svec, S. Eeltink, Nanostructured porous polymer monolithic columns for capillary liquid chromatography of peptides, J. Chromatogr. A. 1374 (2014) 171–179. doi:10.1016/j.chroma.2014.11.063.

[15] L.R. Snyder, J.W. Dolan, High-performance gradient elution: The practical application of the linear-solvent-strength model, Wiley, Hoboken, NJ, USA, 2007.

[16] J.C. Giddings, Sample dimensionality: A predictor of order-disorder in component peak

distribution in multidimensional separation, J. Chromatogr. A. 703 (1995) 3–15.

[17] J.M. Davis, P.W. Carr, Effective saturation: A more informative metric for comparing peak separation in one- and two-dimensional separations, Anal. Chem. 81 (2009) 1198–1207.

[18] J.M. Davis, J.C. Giddings, Origin and characterization of departures from the statistical model of component-peak overlap in chromatography, J. Chromatogr. A. 289 (1984) 277–298.

[19] U.D. Neue, Theory of peak capacity in gradient elution, J. Chromatogr. A. 1079 (2005) 153–161.

[20] H. Liu, J.W. Finch, J.A. Luongo, G.Z. Li, J.C. Gebler, Development of an online two-dimensional nano-scale liquid chromatography/mass spectrometry method for improved chromatographic performance and hydrophobic peptide recovery, J. Chromatogr. A. 1135 (2006) 43–51.

[21] H. Liu, J.W. Finch, M.J. Lavallee, R.A. Collamati, C.C. Benevides, J.C. Gebler, Effects of column length, particle size, gradient length and flow rate on peak capacity of nano-scale liquid chromatography for peptide separations, J. Chromatogr. A. 1147 (2007) 30–36.

[22] M. Gilar, U.D. Neue, Peak capacity in gradient reversed-phase liquid chromatography of biopolymers. Theoretical and practical implications for the separation of oligonucleotides, J. Chromatogr. A. 1169 (2007) 139–150.

[23] N. Marchetti, A. Cavazzini, F. Gritti, G. Guiochon, Gradient elution separation and peak capacity of columns packed with porous shell particles, J. Chromatogr. A. 1163 (2007) 203–211.

[24] X. Wang, D.R. Stoll, A.P. Schellinger, P.W. Carr, Peak capacity optimization of peptide

separations in reversed-phase gradient elution chromatography: Fixed column format, Anal. Chem. 78 (2006) 3406–3416.

[25] P. Petersson, A. Frank, J. Heaton, M.R. Euerby, Maximizing peak capacity and separation speed in liquid chromatography, J. Sep. Sci. 31 (2008) 2346–2357.

[26] J. Courtois, M. Szumski, E. Byström, A. Iwasiewicz, A. Shchukarev, K. Irgum, A study of surface modification and anchoring techniques used in the preparation of monolithic microcolumns in fused silica capillaries, J. Sep. Sci. 29 (2006) 14–24.

[27] S. Eeltink, J.M. Herrero-Martinez, G.P. Rozing, P.J. Schoenmakers, W.T. Kok, Tailoring the morphology of methacrylate ester-based monoliths for optimum efficiency in liquid chromatography, Anal. Chem. 77 (2005) 7342–7347.

[28] S. Wouters, T. Hauffman, M.C. Mittelmeijer-Hazeleger, G. Rothenberg, G. Desmet, G. V. Baron, S. Eeltink, Comprehensive study of the macropore and mesopore size distributions in polymer monoliths using complementary physical characterization techniques and liquid chromatography, J. Sep. Sci. 39 (2016) 4492–4501.

[29] R.R. Walters, J.F. Graham, R.M. Moore, D.J. Anderson, Protein diffusion coefficient measurements by laminar flow analysis: Method and applications, Anal. Biochem. 140 (1984) 190–195.

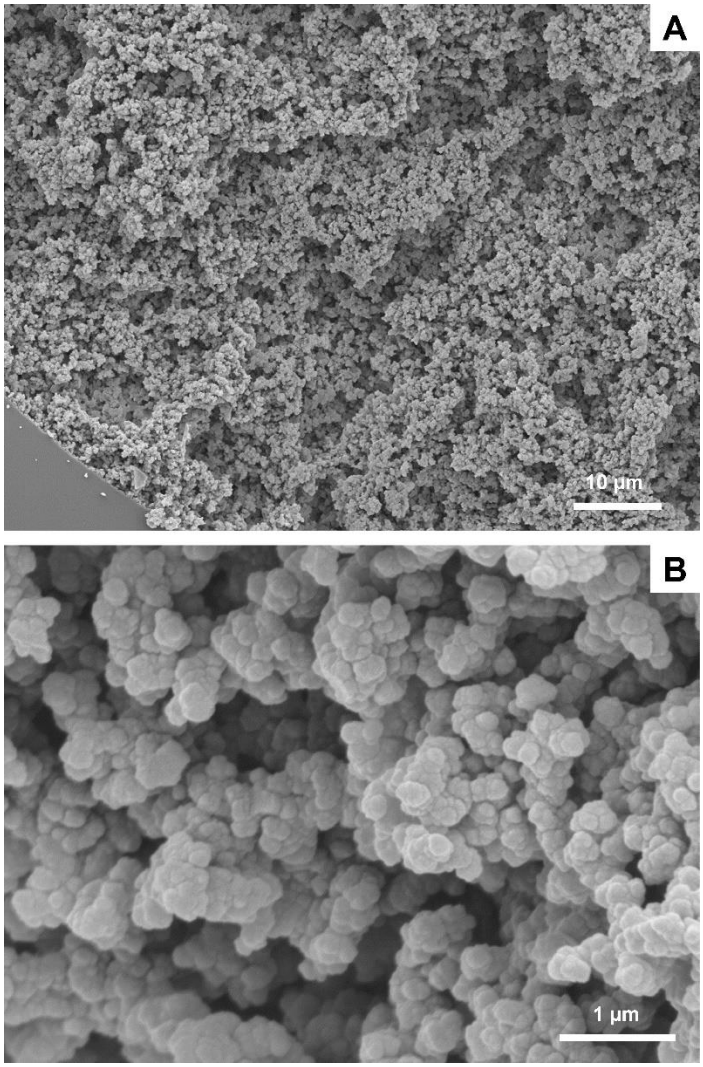

Figure 1. Scanning electron microscopy (SEM) images of the cross section of a 200 µm i.d. monolithic poly(styrene-*co*-divinylbenzene) capillary column (A) prepared by thermal initiation at 70°C and composed of a monomer to porogen ratio of 40:60 wt% and a zoom-in (B).

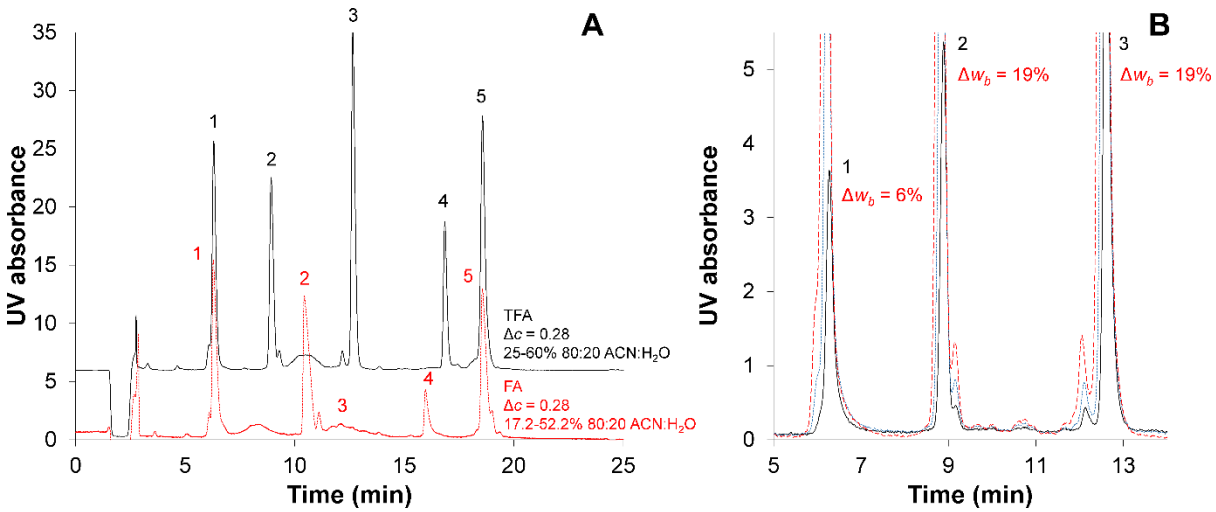

Figure 2. (A) Separation of (1) ribonuclease A, (2) insulin, (3) lysozyme, (4) myoglobin, and (5) carbonic anhydrase, applying a mobile phase A consisting of 0.1% (v/v) aqueous TFA (black chromatogram) or FA (red dotted chromatogram) and mobile phase B of 80:20% (v/v) ACN:H_2O with 0.08% (v/v) TFA or FA; with a gradient window from 25 to 60% of B when TFA was used, or from 17.2 to 52.2% of B when FA was used (B) Zoom-in of peak profiles of (1) ribonuclease A, (2) insulin, and (3) lysozyme, obtained when injecting protein concentration of 2.5 ppm (black), 5 ppm (blue), and 10 ppm (red), applying a mobile phase A consisting of 0.1% (v/v) aqueous TFA and mobile phase B of 80:20% (v/v) ACN:H_2O with 0.08% (v/v) TFA, gradient window from 25 to 60% of B, injection volume of 1 µL, column temperature at 37ºC, and detection at 210 nm. The Δw_b refers to the difference in the peak width at the base, between the protein concentration of 10 and 2.5 ppm.

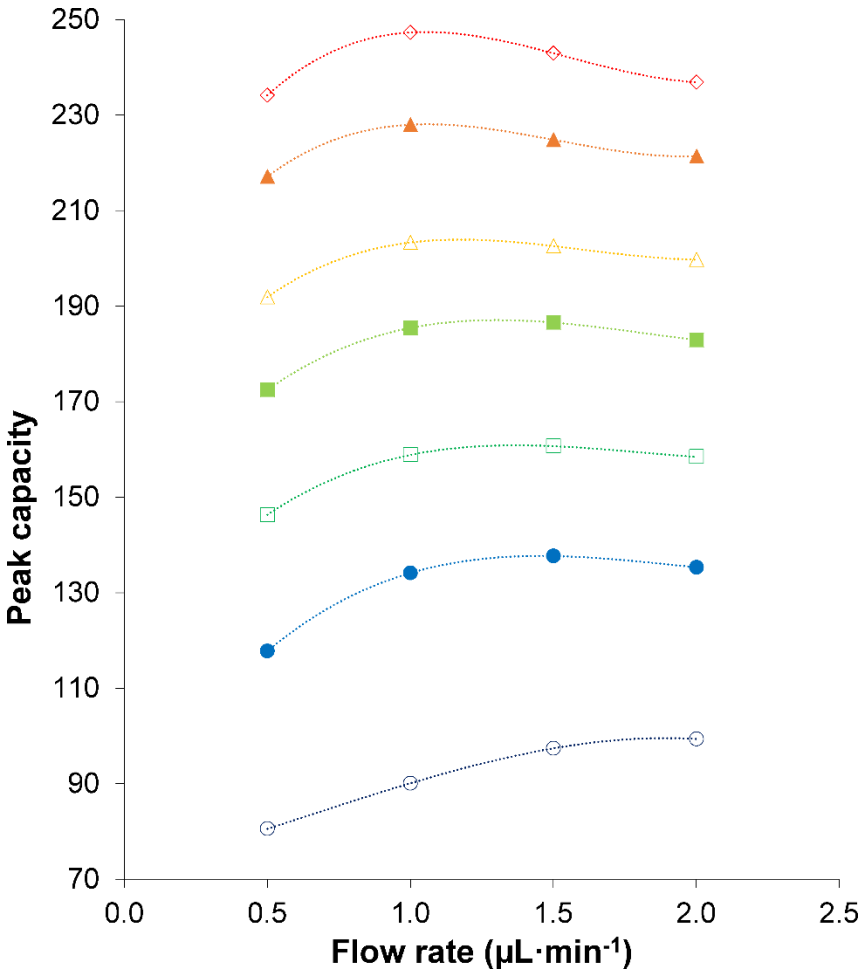

Figure 3. Effect of gradient time and flow rate on the average peak capacity (A) measured on a 200 µm i.d. × 100 mm long monolithic poly(styrene-*co*-divinylbenzene) capillary column. (B) show depicts the effect for individual proteins (carbonic anhydrase, ribonuclease A, and insulin) on peak capacity, showing that F_{opt} is affected by the molecular mass. Experimental conditions similar as in Fig. 2B with 0.1% TFA in the mobile phase. The average peak-capacity values were calculated using equation $n_c = (t_G/W_b) + 1$, applying gradient times of 10 min. (○), 20 min. (●), 30 min. (□), 45 min. (■), 60 min. (△), 90 min. (▲), 120 min. (◊).

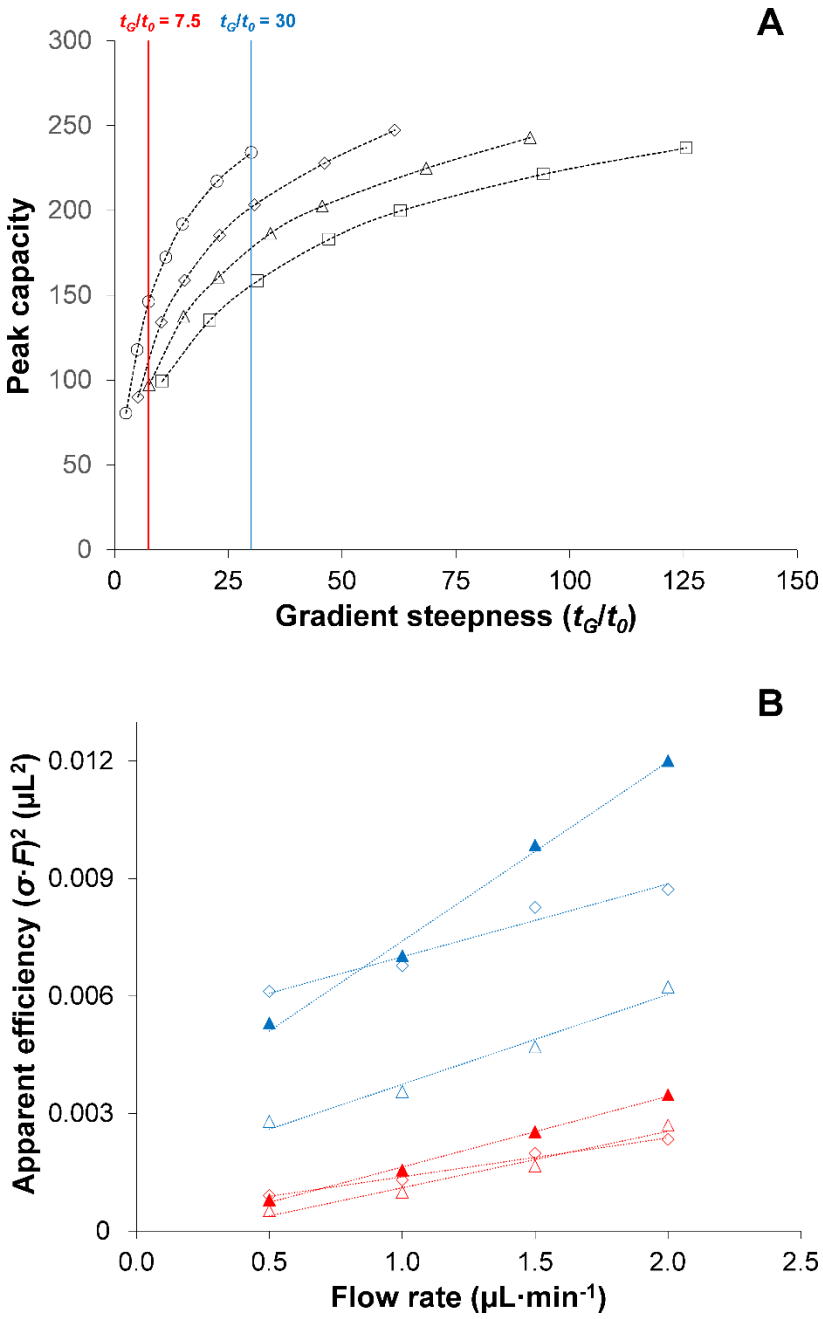

Figure 4. Effect of gradient volume on separation performance as function of flow rate. (A) Shows the average peak capacity as function of t_G/t_0 employing different flow rates: 0.5 µL·min^{-1} (circles), 1.0 µL·min^{-1} (diamonds), 1.5 µL·min^{-1} (triangles), 2.0 µL·min^{-1} (squares). The vertical lines indicate performance data for t_G/t_0 = 7.5 and 30, respectively. (B) Depicts the effect of diffusion coefficients of intact proteins on apparent efficiency (*C*-term effect) as a function of flow rate for t_G/t_0 = 7.5 and 30. Solid triangles = carbonic anhydrase, open triangles

= ribonuclease A, open diamonds = insulin. Experimental conditions similar as in Fig. 2B with 0.1% TFA in the mobile phase.

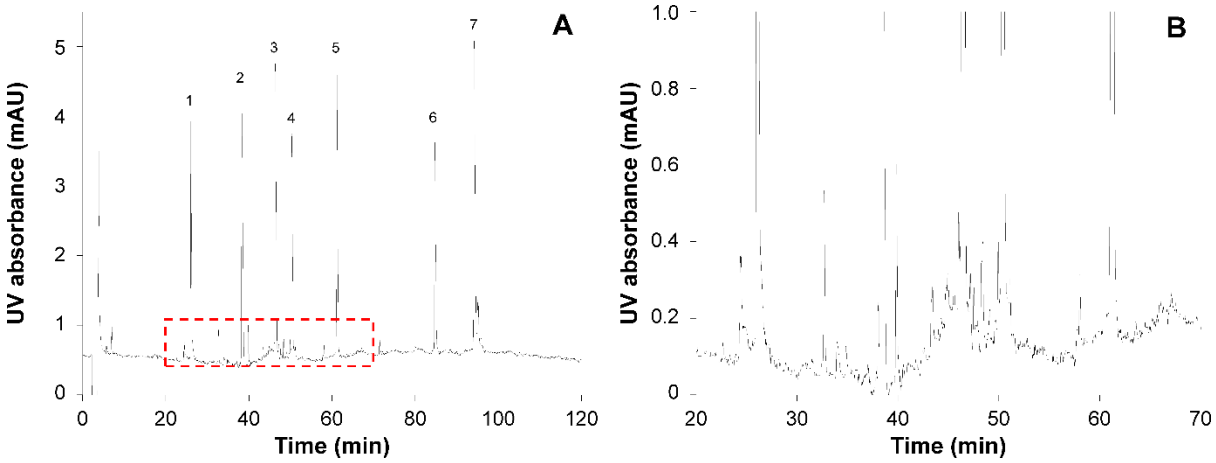

Figure 5. Separation of a mixture of intact proteins and its degradation products at a flow rate of 1 µL·min^{-1} and gradient time of 120 min with Δc = 0.28 and a column temperature at 37°C (A) and a zoom-in of the peak profiles (B). Peak identification: (1) ribonuclease A, (2) insulin, (3) cytochrome *c* equine, (4) cytochrome *c* bovine, (5) lysozyme, (6) myoglobin, and (7) carbonic anhydrase.

Supplementary material

The frequency distribution of the globule size and pore diameter depicted in Fig. S1 was estimated based on scanning electron micrographs. Cross sections of monolithic capillary columns were sputtered with 6 nm of Pt-Pd using a 208 HR sputter coater equipped with a Cressington mtm 20 Thickeness Controller (Cressington Scientific Instruments, Watford, UK). A JSM-6400 field emission scanning electron microscope (JEOL, Tokyo, Japan) was operated at acceleration voltages of 5 kV.

To determine the globule sizes, the SEM pictures were uploaded in ImageJ (NIH, USA) and straight lines ($n \geq 100$), corresponding to the diameter of the globules were manually drawn. The length of the straight lines was subsequently analyzed via the software. This procedure was repeated to determine the macropore size. Note, that this is only a rough estimation of the characteristic feature size.

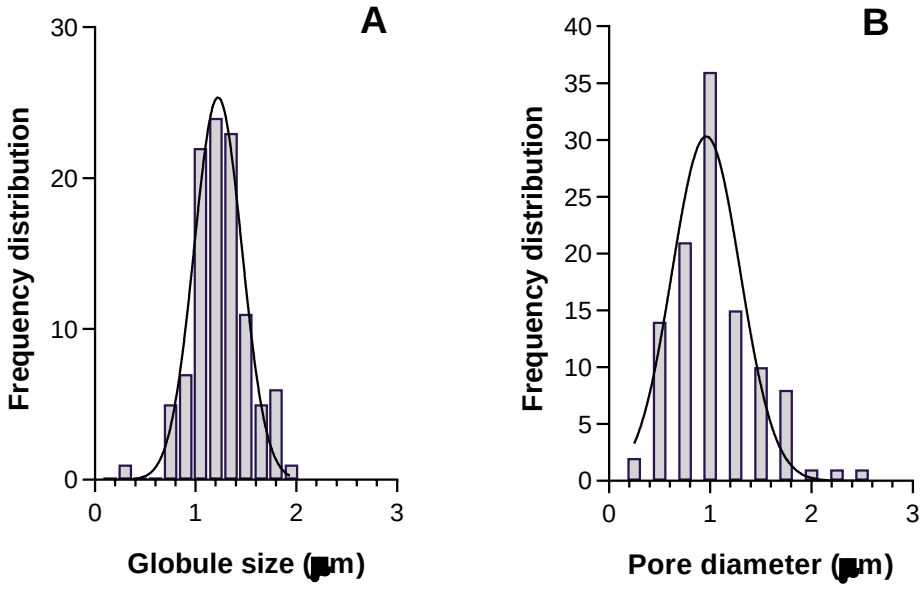

Figure S1. Frequency distribution of the globule size (A) and pore diameter (B) estimated based on scanning electron micrographs (SEM), obtained from $n \geq 100$. The line shows a fitted Gaussian distribution based on the frequency distribution with 95% confidence interval.

The separation efficiency as function of flow rate (van Deemter curve) was recorded by injecting uracil as the t_0-marker applying a mobile phase of 80:20% (v/v) ACN:H_2O, see Fig. S2. Note the experimental was set-up to minimize the extra-column dispersion, *i.e.* using a 4 nL injection valve, the column directly connected at the stator, and applying a 3 nL UV flow cell. The van Deemter curve representing a protein was constructed by reducing the plate height based on the domain size (sum of the mode globule and macropore size) of the monolithic column and applying the diffusion coefficient of a protein with a molecular weight of 22.7 kDa. This corresponds to a diffusion coefficient of 9×10^{-11} $m^2 \cdot s^{-1}$, based on the methodology of laminar flow analysis [1]. Based on this transformation it can be observed that the optimal flow velocity for a protein is a factor 7 lower than that of a small molecule, *i.e.*, uracil.

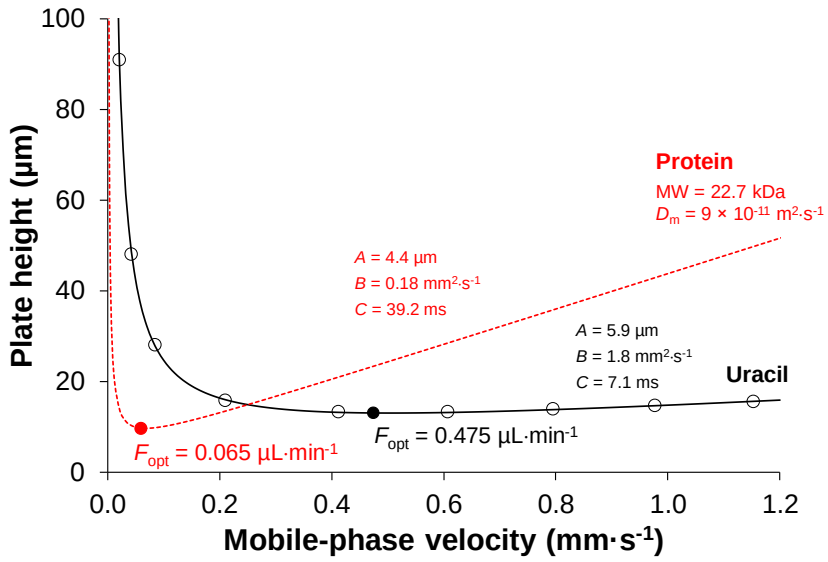

Figure S2. Van Deemter curve recorded for uracil while applying 80:20% (v/v) ACN:H_2O on the poly(styrene-*co*-divinylbenzene) monolithic column. The van Deemter curve for the protein was reconstructed considering the difference in molecular diffusion coefficient.

Fig. S3 shows the ln k vs. ϕ plots of insulin and carbonic anhydrase recorded in isocratic mode applying a flow rate of 1.5 µL·min^{-1}. The S value is analyte depended and is the slope of this curve.

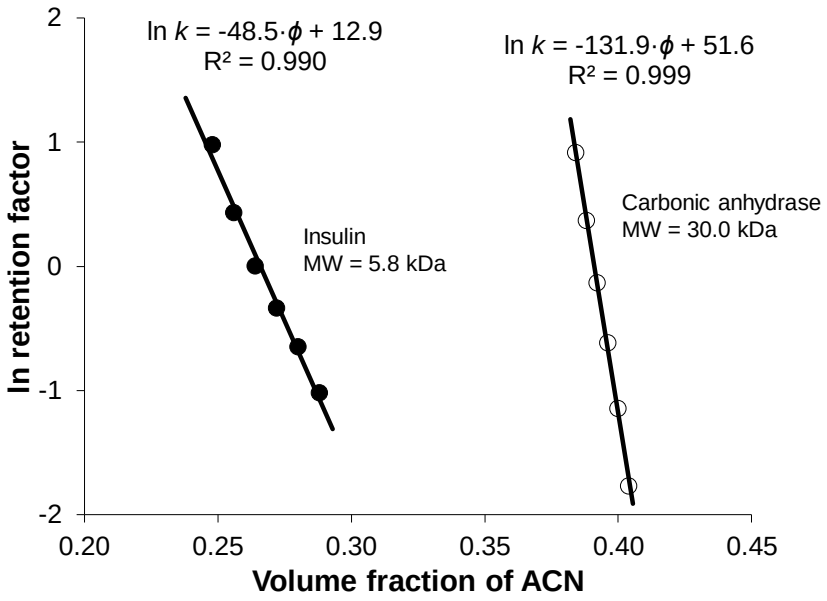

Figure S3. Plots of natural logarithm of retention factor (ln k) as function of the volume fraction, ϕ, of ACN in the mobile phase of insulin (closed symbols) and carbonic anhydrase (open symbols).

Fig. S4 shows the experimental peak capacity recoreded for intact proteins on a monolithic column as function of flow rate and gradient time. The peak capacty was calculated according $n_c = t_G/W + 1$.

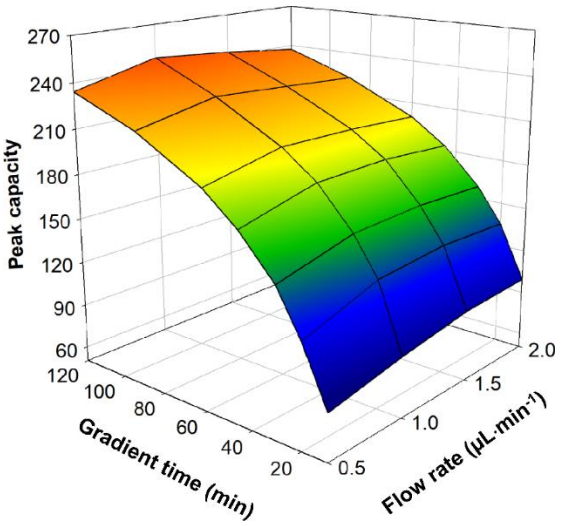

Figure S4. The experimental peak capacites recorded on a poly(styrene-*co*-divinylbenzene) monolithic column as function of flow rate and gradient time using 0.1% TFA as ion pairing agent.

Fig. S5 shows the fit of experimental data applying Neue's model (Eqs. 1 and 2 in the main manuscript). While a reasonable first estimation was obtained for carbonic anhydrase the experimental values for insulin were significantly higher than that predicted with Neue's model. This may be due to an underestimation of the magnitude of the *S* value. When doubling the *S* value for insulin 48.5 (experimentally determined) to 97 to fit appears more the fit appears to be a better predictor.

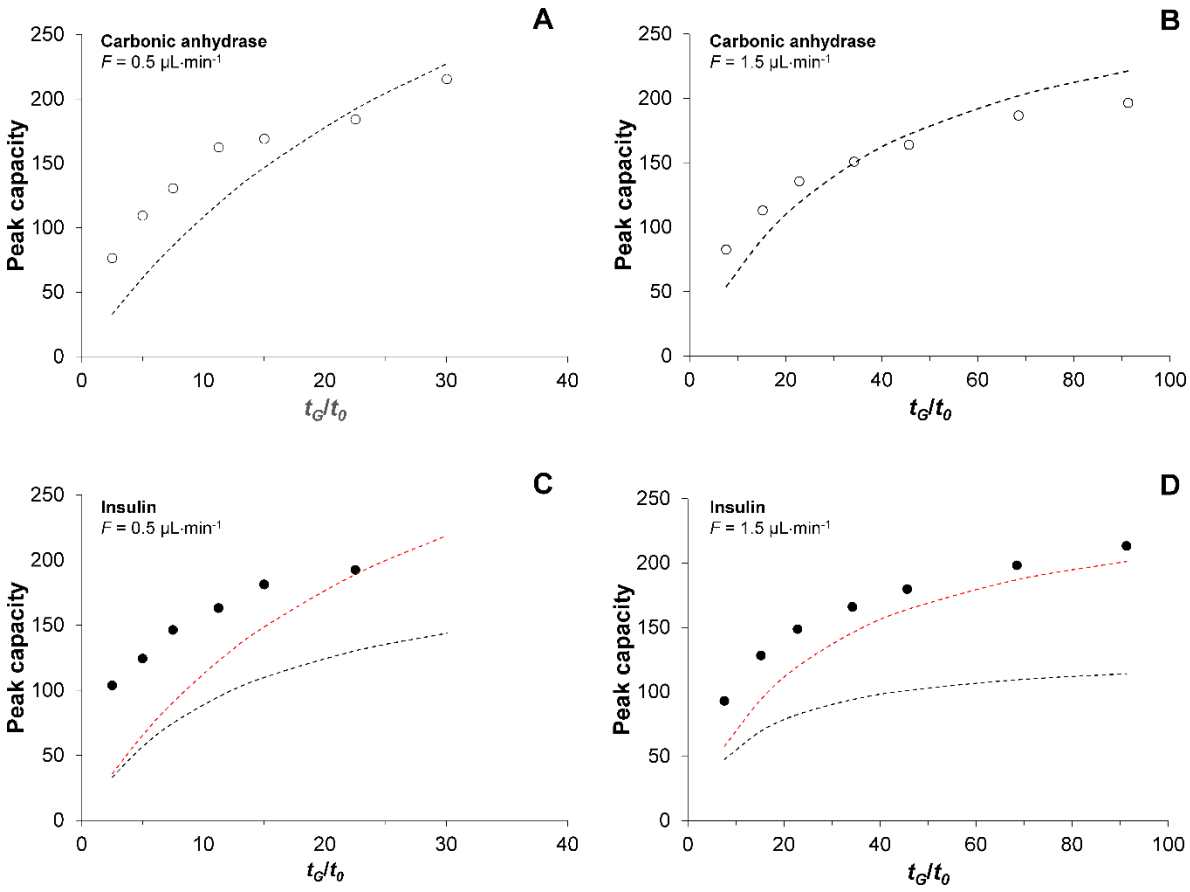

Figure S5. Experimental peak capacity data for carbonic anhydrase and insulin applying flow rates of 0.5 and 15 µL·min$^{-1,}$ respectively. The black fits (dotted lines) were obtained applying S values experimentally determined and reported in Fig S3. The red fit (dotted line for insulin only) was obtained by doubling the experimental *S* value.

Fig. S6 shows the gradient performance for individual proteins as function of flow rate visualizing the effect of mass-transfer (C-term) contribution to the efficiency in gradient mode. Note that the molecular-diffusion coefficients do not directly correlate to the apparent efficiency

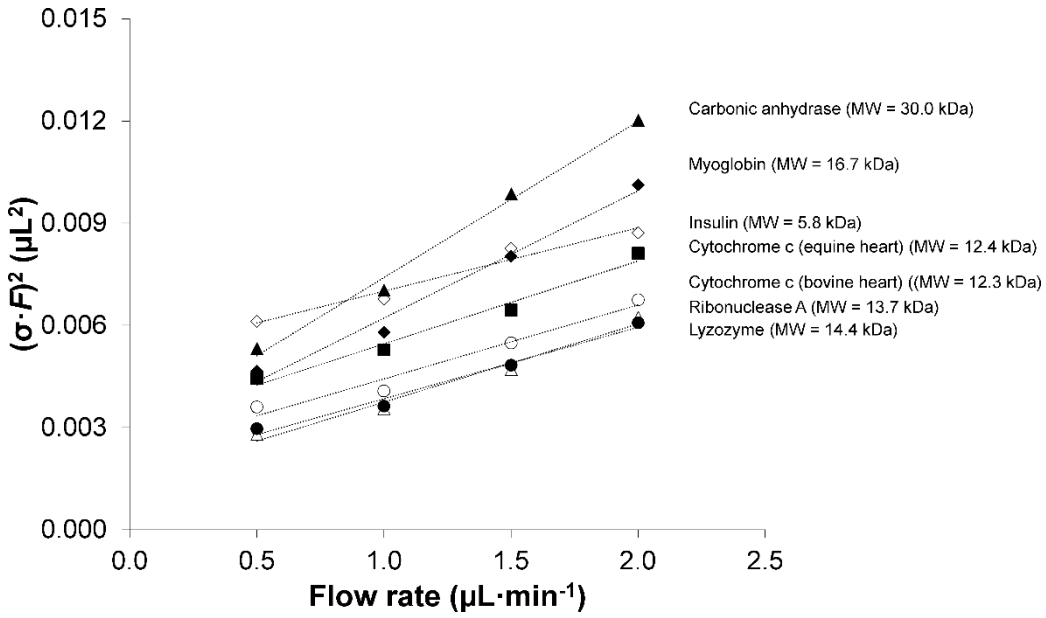

Figure S6. Effect of flow rate on apparent efficiency, corresponding to the volumetric peak variance, as measured in gradient mode for individual proteins

Reference

[1] R.R. Walters, J.F. Graham, R.M. Moore, D.J. Anderson, Protein diffusion coefficient measurements by laminar flow analysis: Method and applications, Anal. Biochem. 140 (1984) 190–195